

COMPRESSION BEHAVIOUR OF FIBRE BUNDLES WITH GRAFTED CARBON NANOTUBES

Stepan V. Lomov*, Larissa Gorbatikh, Ignaas Verpoest

Department MTM, Katholieke Universiteit Leuven, Kasteelpark Arenberg 44, 3001, Leuven, Belgium

**Stepan.Lomov@mtm.kuleuven.be*

Keywords: carbon nanotubes; textile reinforcements; compressibility.

Abstract

When carbon nanotubes (CNTs) are grown on carbon fibres, with the goal to increase toughness of a carbon fibre reinforced composite, the compressibility of the carbon fibre bundle or a fabric decreases significantly. The pressure, necessary to achieve the desired fibre volume fraction in a composite, should be increased by several bars. The paper proposes modelling approaches for calculation of the change of compression resistance of the CNT-grafted fibre bundle and fabric.

1 Introduction

Growth of carbon nanotubes (CNT) or carbon nanofibres (CNF) on fibrous substrates is a widely investigated method for introduction of nano-reinforcements in fibre reinforced composites (FRC). The nano-engineered FRC (nFRC) exhibit significantly improved toughness properties such as the fracture toughness, the interlaminar shear strength and the load threshold for damage initiation [1-3]. The successful developments of tough nFRC have drawn attention to manufacturability of these composites. We discovered [4] that the random “forests” of CNT/CNFs on carbon fibres are not easily compressible, this is in spite of the seemingly flexible and deformable thin and long CNT/CNFs, which, when in contact, have very low friction between them. To regain the targeted fibre volume of the composite after CNT/CNF grafting, the compaction pressure has to be increased by several bars in comparison with the compaction pressure for a “virgin” preform (which lies in the range from 1 bar for vacuum infusion up to several bars for autoclave or RTM processes). In this paper we propose a model for calculation of the compression resistance of a random CNT assembly, which is further used as a building block in a model of compression of a bundle of unidirectionally (UD) arranged fibres (carbon fibres in most of applications) with CNT random forest grown on or between them. Once the compression of a fibre bundle is calculated, the predicted compression diagram can be used as input for deformation models of textile preforms (compression, shear, tension). This upgrades the hierarchical scale of the model to the nano-micro-meso chain, with subsequent use of it in macro-scale simulations of composite forming processes. This paper outlines the mathematics of the models. The reader is referred to a full description of the models and the experimental data in [4-7].

2. Compressibility of a CNT assembly

We consider multiwall CNTs (MWCNT) with diameter of the outer wall d , number of walls N , inter-wall distance $\delta_w = 0.34$ nm. CNTs in the assembly are mechanically represented by fibres with diameter d and certain bending rigidity. The length of the CNT is assumed to be much larger than the distance between contacts of CNTs in the assembly. The CNTs have a curved shape; the orientation of the local tangent $\mathbf{t}(t_x, t_y, t_z)$ to the centre line of the CNT is given by angles φ and θ : $t_x = \cos \varphi \sin \theta$; $t_y = \sin \varphi \sin \theta$; $t_z = \cos \theta$; $0 \leq \varphi \leq \pi$; $0 \leq \theta \leq \pi$

where the z -axis of the Cartesian coordinate system xyz corresponds to the direction of the compression loading of the assembly. The orientation distribution function (ODF) $\Omega(\varphi, \theta)$ gives the probability of \mathbf{t} belonging to an element of a unit sphere $d\varphi \cdot \sin \theta d\theta$ and is

normalised as $\int_0^\pi d\varphi \int_0^\pi \Omega(\theta, \varphi) \sin \theta d\theta = 1$. As an example a 3D-uniform distribution will be

considered. In this case $\Omega(\varphi, \theta) = \frac{1}{2\pi}$.

A bulk density ρ is the main measurable parameter of the CNT assembly, directly related to the volume fraction of the CNT in it. The density of MWCNT wall is $\rho_w = 2$ g/cm³, referring to the wall volume defined by the inter-wall distance $\delta_w = 0.34$ nm. The volume fraction of the fibres (considered as solid curved rods) with the diameter d representing the CNT is calculated as

$$V_f = \frac{\rho}{\rho_w} \cdot \frac{1}{1 - \left[1 - (N-1) \frac{2\delta_w}{d} \right]^2}$$

For the characteristic value $\rho = 0.3$ g/cm³, $V_f = 0.17$.

The mechanical properties of the CNTs in the assembly are characterised by their bending rigidity. The initial bending rigidity B_0 of a single wall (SWCNT) or multiwall (MWCNT) carbon nanotubes is calculated as follows:

$$B_0 = E_w \cdot \frac{\pi}{64} (D_{out}^4 - D_{in}^4) = E_w \cdot Y; Y = \frac{\pi}{64} (D_{out}^4 - D_{in}^4); D_{out} = d; D_{in} = D_{out} - 2 \cdot \delta_w \cdot (N - 1)$$

where E_w is the Young modulus of the CNT wall, corresponding to the wall thickness equal to the inter-wall distance δ_w , Y is the moment of inertia of the CNT cross-section, D_{out} and D_{in} are diameters of the outer and the inner walls. It is assumed that interactions between the CNT walls are negligible in comparison with the resistance provided by deformation of the elementary tubes ("sword-in-sheath" effect). For the typical parameters of the MWCNT $B_0 = 7.77 \cdot 10^6$ nN·nm². The value of $E_w = 1$ TPa is introduced here as a "rule of thumb" theoretical value often assumed in the mechanical calculations of CNT.

When a hollow tube is bent, after certain critical point it loses stability and buckles. This phenomenon for CNTs has been studied experimentally and numerically [8,9], and the following criterion for buckling has been established: the CNT buckles when $\kappa > \kappa_b$ where κ is the curvature of the mid-line of the CNT. A formula $\kappa_b = A/d^2$ has been proposed in [9] for calculation of the critical value κ_b with $A = 0.064$ nm for SWCNT and $A = 0.048$ nm for DWCNT [8]. The curvature is calculated as

$$\kappa = \arcsin \frac{q}{b} / (2b)$$

where b is the half-length of the CNT, q is the bending deflection. Hence the critical deflection q_b for onset of the buckling can be calculated as

$$q_b = b \sin\left(2 \frac{A b}{d d}\right)$$

When the buckling state is reached, the effective bending rigidity of the CNT drops, and after that the bending moment stays approximately constant with the increase of the curvature. This leads to the formula for dependency of the CNT tangent bending rigidity on the curvature:

$$B(\kappa) = \begin{cases} B_0, & \kappa < \kappa_b; \\ \alpha B_0, & \kappa = \kappa_b; \\ \alpha B_0 \frac{\kappa_b}{\kappa}, & \kappa > \kappa_b \end{cases}$$

where $B(\kappa)$ is the bending rigidity, corresponding to the curvature κ , α is the coefficient of decrease of the bending rigidity on the onset of buckling (**Error! Reference source not found.**). The experimental data and calculations in [8] suggest that $\alpha \approx 0.5$ can be adopted as a reasonable value for different cases of CNT diameter, number of walls and chirality.

The friction between CNTs is characterised by the friction coefficient μ and adhesion force F_{adh} : friction force F_{frict} for a given normal force F_n is calculated as $F_{frict} = \mu(F_n + F_{adh})$. Measurements and atomistic modelling in [10-12] suggest as characteristic values $\mu=0.005$ and $F_{adh}=1$ nN.

The description of the geometry of a random CNT assembly follows the approach, developed for fibrous assemblies in [13]. Average distance between the contacts b is calculated, based on the probability of contact between the fibres, as

$$b = \frac{V}{2dLI} = \frac{\pi}{8} d \frac{1}{V_f I},$$

where V is the volume of the assembly, L is the total length of the fibres in the assembly, and the orientation averaging is represented by integral I , which is calculated as

$$I = 2 \int_0^{\pi} d\varphi \int_0^{\pi/2} J(\theta, \varphi) \Omega(\theta, \varphi) \sin \theta d\theta; J(\theta, \varphi) = 2 \int_0^{\pi} d\varphi' \int_0^{\pi/2} \Omega(\theta', \varphi') \sin \theta' \sqrt{1 - [\cos \theta \cos \theta' + \sin \theta \sin \theta' \cos(\varphi - \varphi')]^2} d\theta'$$

The factors “2” and integration from 0 to $\pi/2$ appear here because of symmetry of the ODF $\Omega(\theta, \varphi)$. For uniform ODF $I = \pi/4 = 0.785$. Note that the same symbol is used for the average distance between the contacts and for the half-length of the elementary bent interval of a CNT, which corresponds to the fact that bending of the CNT is the result of contact interactions. For the typical parameters of the CNT assembly $b = 60$ nm. For the following calculations the average projection of the inter-contact interval on the z axis, b_z , is needed. For an individual inter-contact interval $b_z = b \cos \theta$; orientation averaging of this dependency

gives the average value of b_z as $b_z = 4bK$; $K = \int_0^{\pi/2} d\varphi \int_0^{\pi/2} \Omega(\theta, \varphi) \sin \theta \cos \theta d\theta$. For the uniform ODF $K = 0.125$.

The number of contacts between CNTs per unit volume of the assembly n_c is calculated as $n_c = \frac{L}{2bV} = \frac{16}{\pi^2} I \frac{V_f^2}{d^3}$. For the uniform ODF $n_c = 1.27 \frac{V_f^2}{d^3}$, and for the typical assembly parameters assembly $n_c = 4587 \mu\text{m}^{-3}$.

The calculation of the compression resistance of a CNT assembly is based on the approach, developed for fibrous assemblies in [14], We further develop the model [14] to account for phenomena specific to CNT assemblies: buckling of CNT and the exceptionally low friction.

Consider a pressure p which creates forces F on the contact points of the assembly. Fig 1 depicts these forces at a contact point O.

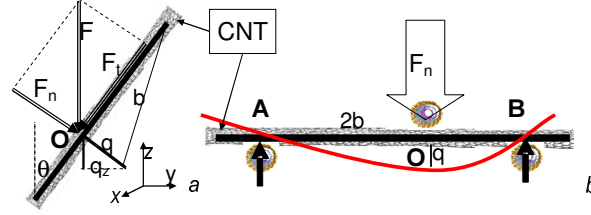


Figure 1 Forces in the contact points: (a) force components and displacement at a contact point O; (b) bending of a fibre at non-sliding contact at point O, supported by the neighbouring contacts at points A and B.

We assume that the resultant forces at all the contact points have a vertical (z) direction. Consider a volume of the assembly with dimensions $l_x l_y b_z$ (thickness corresponding to the average projection on z -axis of the mean distance between contacts). Following [14], we assume that the pressure p is evenly distributed over the contacts in this volume, and the mean force at the contact point is calculated as

$$F_{mean} = \frac{P}{n_c b_z} = \frac{\pi}{8} p d^2 \frac{1}{V_f K}$$

For the typical assembly and $p = 1$ bar $F_{mean} = 0.74$ nN.

Slipping at a contact will occur if $F_t > F_{frict}$. Let θ be the orientation of the fibre under consideration. The scheme of Fig 1 shows that the slipping condition can be written as

$$F_t > F_{frict} \Rightarrow F \sin \theta > \mu (F \cos \theta + F_{adh})$$

Using F_{mean} as a value of the contact force, this condition leads to the following condition for slipping:

$$\theta < \theta_{slip} = \arctan \frac{1}{\mu} - \arcsin \frac{\mu F_{adh}}{F \sqrt{1 + \mu^2}}$$

For the typical assembly and $p = 1$ bar $\theta_{slip} = 89.3^\circ$. The very high value of the slipping threshold is the result of a very low friction coefficient. This feature distinguishes the CNT assembly from fibrous assemblies dealt with in the previously developed models for non-woven textile materials.

The proportion of slipping (c_{slip}) and non-slipping ($c_{non-slip}$) contacts in the assembly is calculated as

$$c_{slip} = 4 \int_0^{\pi/2} d\varphi \int_0^{\theta_{slip}} \Omega(\theta, \varphi) \sin \theta d\theta = 2\pi \int_0^{\theta_{slip}} \Omega(\theta, \varphi) \sin \theta d\theta; c_{non-slip} = 1 - c_{slip}$$

For the typical assembly and $p = 1$ bar $c_{slip} = 0.9950$. This gives the number of non-slipping contacts as $24 \mu\text{m}^{-3}$ out of $4587 \mu\text{m}^{-3}$ in total.

Consider first a slipping contact. The force F can be calculated from

$$F \sin \theta = \mu F \cos \theta + \mu F_{adh} \Rightarrow F = \frac{\mu F_{adh}}{\sin \theta - \mu \cos \theta}$$

The average force on the slipping contacts F_{slip} will be

$$F_{slip} = \mu F_{adh} \frac{2\pi \int_0^{\theta_{slip}} \frac{1}{\sin \theta - \mu \cos \theta} \Omega(\theta, \varphi) \sin \theta d\theta}{c_{slip}}$$

For a uniform ODF and $\mu \ll 1$: $F_{slip} \approx \mu F_{adh}$.

The average force on non-slipping contacts $F_{non-slip}$ will be calculated from the assumption of even distribution of the pressure among slipping and non-slipping contacts.

$$F_{mean} = c_{slip} F_{slip} + (1 - c_{slip}) F_{non-slip} \Rightarrow F_{non-slip} = \frac{F_{mean} - c_{slip} F_{slip}}{1 - c_{slip}}$$

For the typical assembly and $p = 1$ bar, $F_{mean} = 0.74$ nN, $F_{slip} = 0.005$ nN, $F_{non-slip} = 98$ nN.

Fig 1b shows a scheme of loading of a CNT at a non-slipping contact at point O. The CNT is bent under the normal component of the force F_n as an elastic beam with float $2b$, freely supported at the ends A and B – neighbouring contacts (which can be slipping or non-slipping). If the CNT does not buckle, then the deflection in the direction of normal force is

calculated as $q = \frac{b^3}{kB} F_n$, where k depends on the place of application of the force, and B is the bending rigidity of the CNT. Assuming that the force is applied in the centre of the float, and the CNT is straight between the contacts, $k = 24$. For the force in non-slipping contacts of 98 nN, estimated above, the deflection q is estimated as 0.11 nm.

Introducing the bending equation into the buckling condition and using the average value of the force at the slipping contact to calculate the normal force $F_n = F_{non-slip} \cos \theta$, one arrives to a threshold value of the orientation θ_{buckle} : buckling occurs if

$$\theta > \theta_{buckle}; \quad \sin \theta_{buckle} = \frac{kB_0}{F_{non-slip} b^2} \sin \left(\frac{2Ab}{d^2} \right)$$

Accounting for possible buckling of the CNT, the z-projection q_z of the deflection at a non-slipping contact with orientation of the CNT given by the angle θ is calculated as

$$q_z(\theta) = \frac{b^3}{kB(\theta)} F \sin^2 \theta; B(\theta) = B_0 \beta(\theta); \beta(\theta) = \begin{cases} 1, & \theta < \theta_{buckle} \\ \alpha \frac{\theta_{buckle}}{\theta}, & \theta \geq \theta_{buckle} \end{cases}$$

When an increment of pressure Δp is applied, resulting in the pressure p , and assuming that the sliding contacts are restricted in their movement by the non-sliding contacts, then the

increment of deformation of the assembly can be calculated as $\Delta \varepsilon = \frac{\Delta q_z}{b_{z0}}$, where

subscript 0 corresponds to the non-deformed configuration, and the average z-projection of the displacement Δq_z under an increment of the force $\Delta F_{non-slip}$ (caused by an increment of the applied pressure Δp) is calculated by orientation averaging:

$$\Delta q_z = \frac{b^3 \Delta F_{non-slip}}{kB_0} \frac{2\pi \int_{\theta_{slip}}^{\pi/2} \frac{1}{\beta(\theta)} \Omega(\theta, \varphi) \sin \theta \sin^2 \theta d\theta}{(1 - c_{slip})}$$

The compression modulus is calculated as $E = \Delta p / \Delta \varepsilon$. After the load increment the

deformation will reach a value ε , and the volume fraction of fibres/CNT will be $V_f = \frac{V_{f0}}{1 - \varepsilon}$.

Using formulae from [15], the ODF $\Omega(\theta, \varphi)$ after a compression deformation ε can be calculated using initial ODF $\Omega_0(\theta, \varphi)$ as

$$\Omega(\theta, \varphi) \sin \theta = \Omega_0(\theta_0, \varphi) \sin \theta_0 \frac{H \sec^2 \theta}{1 + H^2 \tan^2 \theta}; \quad \sin \theta_0 = \sqrt{\frac{H^2 \tan^2 \theta}{1 + H^2 \tan^2 \theta}}; \quad H = 1 - \varepsilon;$$

3. Compression of a fibre bundle

We consider a bundle of fibres. The shape of the bundle cross section is not important – the bundle can be a round or elliptical yarn, a flat roving etc. The bundle has a certain resistance to compression, which can be characterised by a compression diagram “thickness vs pressure”. This compression curve of a virgin fibre bundle is assumed to be known. The model calculates *the change* of the compression curve after a random assembly of CNTs is grown on the fibres. Two possible morphologies of the CNT growth will be considered (Fig 2): a random CNT “forest” concentrated near the surface of the fibres (“S-model”) and a random CNT assembly homogeneously filling the volume between the fibres (“V-model”). The real morphology is a combination of the S-and V-models.

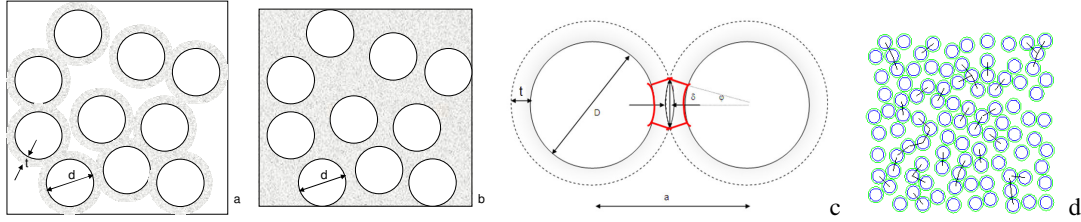


Figure 2 Two schematic configurations of CNT-grafted fibre bundle and Interaction of CNT-grafted fibres in S-model: (a) S-model; (b) V-model; (c) a pair of interacting fibres; (d) random realisation of 100 CNT-grafted fibres, $V_f=0.4$, $t = 1 \mu\text{m}$. Lines show fibre pairs with compressed CNT layer.

For the **V-model** The fibre volume fraction in the bundle is calculated as $V_f = \frac{T}{w\rho_f h}$, where

T is the linear density, w – initial width and h – thickness of the bundle. Assuming a uniform distribution of the CNTs in the inter-fibre volume, the initial average density of the CNT assembly is calculated as $\rho_G^V = \frac{\rho_f V_f m_G}{1 - V_f}$. Applying the model of compression of a random

CNT assembly, described in the previous section, the compression diagrams $\varepsilon_G(p)$ of the inter-fibre CNT assembly are calculated. The compression diagram of the grafted bundle is calculated based on the assumption: the pressure acting on the inter-fibre CNT assembly and on the assembly of fibres in the bundles is the same as the pressure applied to the grafted bundle (“hydrostatic Pascal law”). Under this assumption

$$h_G(p) = h_f(p) + (h_G(0) - h_f(0)) \cdot (1 - \varepsilon_G(p))$$

where $h_G(p)$ is the compression diagram of the grafted bundle, $h_f(p)$ is the compression diagram of the virgin bundle.

In stead of a uniform distribution of the CNTs in the inter-fibre space, the **S-model** assumes that the CNT are concentrated in layers with thickness t around the fibres (Fig 2c,d). In this case the initial average density of the CNT assembly is calculated as

$$\rho_G^s = \rho_f \frac{m_G}{\left(1 + \frac{2t}{D}\right)^2 - 1}$$

The interaction of individual grafted fibres is calculated as follows. We consider two segments of fibres of a unit length in the compressed assembly with the centres at the distance a ($a - D < 2t$) and a CNT “forest” between them (Fig 2c). The fibres lay apart before the compression. We assume that the forest is compressed only in the region bounded by the thick lines in 2b. The volume of this region (per unit length of the fibres) before the compression is designated as v_0 , after the compression as v_1 :

$$v_0 = \frac{1}{2} \varphi (D_1^2 - D^2), v_1 = v_0 - \frac{D_1^2}{2} (\varphi - \sin \varphi \cos \varphi); D_1 = D + 2t; \varphi = \arcsin \sqrt{1 - \left(1 - \frac{\delta}{D_1}\right)^2};$$

where $\delta = \max(0, D_1 - a)$. During the compression the compressive deformation of the CNTs

in the grafting is given by $\varepsilon_G = 1 - \frac{v_1}{v_0}$, and the mechanical work per unit length associated

with the compression of the “forest” by

$$W(a) = W(v_0 \rightarrow v_1) = - \int_{v_0}^{v_1} p(\varepsilon_G) dv = v_0 \int_0^{\varepsilon_G} p(\varepsilon_G) d\varepsilon_G$$

where pressure $p(\varepsilon_G)$ is the inverse of relation $\varepsilon_G(p)$, already calculated above. The next step is to calculate mechanical work $\bar{W}(V_f)$ per unit volume necessary to compress the CNT layers around the fibres for randomly placed fibres with a given fibre volume fraction V_f . Generating

a random realisation of N_f fibres in a volume $A \times A$, $A^2 = \frac{N_f \pi D^2}{4V_f}$, let M be a number of pairs

of fibres, which are sufficiently close for the CNT forests on them to be compressed (see an example in 2d). Then the mechanical energy per unit volume, associated with the compression of the forests, is calculated as

$$\bar{W}(V_f) = \frac{4V_f}{N_f \pi D^2} \sum_{i=1}^M W(a_i)$$

where a_i is the distance between centres of a pair i of the neighbouring fibres. $\bar{W}(V_f)$ can be interpreted as an additional pressure, needed to reach a given fibre volume fraction of the bundle. Then the compression diagram $p_G(h)$ of the CNT-grafted fibre bundle can be calculated as follows:

$$p_G(h) = p_f(V_f(h)) + \bar{W}(V_f(h)) - [p_f(V_f(h_0)) + \bar{W}(V_f(h_0))]$$

where $p_f(h)$ is the compression diagram of the virgin bundle, $V_f(h)$ is calculated using equation (1), and the last term is subtracted to account for the fact that the bundle has thickness h_0 at zero pressure.

4. Conclusion

The mathematical formulation of models of compression of CNT random assembly and a bundle of CNT grafted fibres has been presented. The reader is referred to [4-7] for experimental validation and more details on the models.

Acknowledgement The research is done in the framework of projects “New model-based concepts for nano-engineered polymer composites” funded by K.U.Leuven Research Council (GOA 10/004).

References

1. Qian H, Greenhalgh ES, Shaffer MSP, Bismarck A (2010) Carbon nanotube-based hierarchical composites: a review. *Journal of Materials Chemistry* **20**:4751-4762
2. Chou TW, Gao LM, Thostenson ET, Zhang ZG, Byun JH (2010) An assessment of the science and technology of carbon nanotube-based fibers and composites. *Composites Science and Technology* **70** (1):1-19
3. De Greef N, Gorbatiikh L, Godara A, Mezzo L, Lomov SV, Verpoest I (2011) The effect of carbon nanotubes on the damage development in carbon fiber/epoxy composites. *Carbon* **49**:4650-4664.
4. Lomov SV, Gorbatiikh L, Kotanjac Z, Koissin V, Houille M, Rochez O, Karahan M, Mezzo L, Verpoest I (2011) Compressibility of carbon woven fabric with carbon nanotubes grown on the fibres. *Comp Sci Techn* **71** (3):315–325
5. Lomov SV, Gorbatiikh L, Houille M, Kotanjac Z, Koissin V, Vallons K, Verpoest I (2011) Compression resistance and hysteresis of carbon fibre tows with grown carbon nanotubes/nanofibres. *Composites Science and Technology* **71**:1746-1753
6. Lomov SV, Gorbatiikh L, Verpoest I (2011) A model for the compression of a random assembly of carbon nanotubes. *Carbon* **49**:2079-2091.
7. Lomov SV, Gorbatiikh L, Verpoest I (2011) Compression behaviour of a fibre bundle with grafted carbon nanotubes. *Carbon* **49**:4458-4465
8. Yao XH, Han Q, Xin H (2008) Bending buckling behaviors of single- and multi-walled carbon nanotubes. *Comput Mater Sci* **43** (4):579-590
9. Yakobson BI, Brabec C, Bernholc J (1996) Nanomechanics of carbon tubes: Instabilities beyond linear response. *Phys Rev Lett* **76** (14):2511-2514
10. Lucas M, Zhang X, Palaci I, Klinke C, Tosatti E, Riedo E (2009) Hindered rolling and friction anisotropy in supported carbon nanotubes. *Nature Materials* **8**:876-881.
11. Bhushan B (2008) Nanotribology of carbon nanotubes. *J Phys-Condens Matter* **20** (36)
12. Falvo MR, Taylor RM, Helsen A, Chi V, Brooks FP, Washburn S, Superfine R (1999) Nanometre-scale rolling and sliding of carbon nanotubes. *Nature* **397** (6716):236-238
13. Komori T, Itoh M, Takany A (1992) A model analysis of the compressibility of fibre assemblies. *Textile Research Journal* **62** (10):567-574
14. Lee DH, Lee JK (1985) Initial compressional behaviour of fibre assembly. In: Kawabata S, Postle R, Niwa M (eds) Objective measurement: Applications to product design and process control. *The Textile Machinery Society of Japan*, Osaka, pp 613-622
15. Carnaby GA, Pan N (1989) Theory of the compressional hysteresis of fibrous assemblies. *Textile Research Journal* **59**:275-284